PHILOSOPHICAL TRANSACTIONS OF THE ROYAL SOCIETY A MATHEMATICAL, PHYSICAL & ENGINEERING SCIENCES

Strength, Fracture and Erosion Properties of CVD Diamond [and Discussion]

J. E. Field, E. Nicholson, C. R. Seward, L. M. Brown, J. E. Butler and Z. Feng

Phil. Trans. R. Soc. Lond. A 1993 **342**, 261-275
doi: 10.1098/rsta.1993.0020

Strength, fracture and erosion properties of CVD diamond

By J. E. Field, E. Nicholson, C. R. Seward and Z. Feng†
Cavendish Laboratory, Madingley Road, Cambridge CB3 0HE, U.K.

Theoretical and experimental studies have been made on the effect of high modulus coatings on the stress fields generated by indentation and impact onto a flat half-space. The theoretical work used finite-element techniques and it shows that a high modulus coating can have a significant effect on the maximum tensile stresses generated in the substrate providing there is a good bond at the coating/substrate interface. Because it is technically difficult to deposit layers of more than a few micrometres thickness without residual stresses causing debonding, double and multilayer systems have also been examined theoretically. A variety of techniques have been used to determine the strength, modulus, expansion coefficient, thermal conductivity and other physical properties of chemical vapour deposition CVD diamond layers. These are briefly reviewed and data from our own studies using such techniques as the vibrating reed, bulge test and indentation are present. The erosion properties of both CVD coated substrates and CVD free-standing layers are presented for both liquid drop and solid particle erosion. Finally, a study has also been made of the frictional properties of various CVD diamond layers in a range of environments; data are compared with our earlier work on bulk diamond.

1. Introduction

The strength properties of CVD (chemical vapour deposition) diamond films are of great current interest. Theoretical predictions, of the type outlined in §2, suggest that high modulus coatings should improve the strength, wear and erosion properties of components. However, questions arise about the strength of the interface and the size and nature of residual stresses left by the deposition process. To help with theoretical predictions, any assessment of the practical use of these coatings, and optimization of the CVD processes, it is important to measure properties such as hardness, moduli, Poisson ratio, thermal expansion coefficient and thermal conductivity; all, ideally, as functions of temperature. This paper briefly outlines techniques used for such measurements as well as methods for measuring the performance of CVD coatings in situations involving frictional rubbing, impact, erosion and wear.

2. Effect of a high modulus coating on contact stresses

A finite-element model has been developed by van der Zwaag & Field (1982) for modelling the effect of a high modulus coating on the stress field generated by hertzian contact (sphere on a flat). The coating layer was thin, being no more than 20% of the contact radius of the indent. It is shown that, as expected, the axial

† Present address: Computer Mechanics Laboratory, University of California at Berkeley, U.S.A.

Phil. Trans. R. Soc. Lond. A (1993), **342**, 261–275
Printed in Great Britain

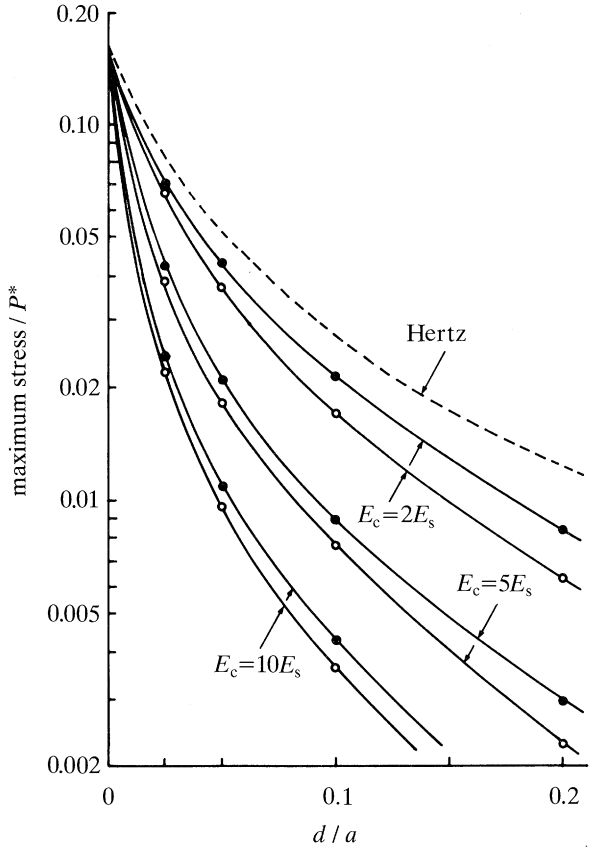

Figure 1. Variation of the maximum radial stress in the substrate with normalized coating thickness for a single layer coating; d is the coating thickness and a the radius of contact. The broken line is the Hertz solution for an isotropic solid (after van der Zwaag & Field 1982). ●, $\nu_c = 0.2$; ○, $\nu_c = 0.3$.

stresses are increased by the presence of the coating but the radial stresses (which can lead to tensile failure) are decreased. In this study, Young's modulus, Poisson's ratio and the thickness of the coating were varied. The results for the maximum tensile (radial) stress generated at the interface are summarized in figure 1. If the half-space were a uniform material then the stress would decrease with depth as shown by the dotted line. The decrease of stress at the depth of the interface, d, is increased dramatically by the high modulus coating; the examples given are for coating moduli, E_c, 2, 5 and 10 times the substrate modulus, E_s. (E_c/E_s for CVD diamond on silicon or zinc sulphide would be *ca.* 6 and 10 times respectively.) The major effects are with modulus and coating thickness, although the effect of Poisson's ratio is also significant. The physical reason that the high modulus coating reduces the build-up of the tensile radial stress is that it restricts the movement (displacement) of the substrate. For this to take place, a good bond between coating and substrate is essential.

As it is technically difficult to deposit layers with a thickness greater than a few micrometres without residual stresses resulting in debonding of the layer, double-layer systems where each layer has different elastic properties have also been investigated (van der Zwaag *et al.* 1986). The individual coating layers were taken as

having equal thickness in this work. A combination of layers was found to be less effective than a thick layer with a modulus equivalent to the greater of the two moduli of the two coating layers. It was found that the order of these coating layers (i.e. whether the top or the bottom layer had the higher modulus) made no difference to the resultant stress in the substrate at the interface between the coating and the substrate. Again the effectiveness of the coating is reduced as the total coating thickness is reduced. There were differences, however, in both the stresses at the top surface of the coating and the interface between the coatings. The stresses in the interlayer are reduced, for example, when the higher modulus layer provides the outer layer of the coating. The surface stresses were again found to be increased for the coated material, the precise value depending on the combination chosen. Experimental work for germanium samples protected by hard carbon layers is given by van der Zwaag & Field (1983*a*).

In summary, it is clear that high modulus coatings have great potential, and also that finite element modelling can play a useful part. What restricts the modelling work at present is a lack of information on the physical properties of the coating, the strength of the bond between the coating and the substrate and the magnitude and sign of the residual stresses left by the deposition process. Important film properties which need to be measured are the hardness, moduli, the Poisson's ratio, the thermal expansion coefficient and the thermal conductivity; all, ideally, as functions of temperature.

3. Thin film property measurement

(*a*) *Hardness*

Typical Vickers micro-indenters are not suitable; however, nano-indenters, or ultramicro-indenters with very fine-scale indenter tips, are. A considerable amount of effort has been expended in interpreting the data and allowing the coating hardness to be evaluated (see, for example, Pethica *et al.* 1983; Isukamoto *et al.* 1987; Oliver & McHargue 1988; McHargue 1990; Smith *et al.* 1992).

(*b*) *Young's modulus*

Essentially four methods are used for this. First, a vibration technique in which a thin beam of substrate material of known properties is vibrated with and without a coating. The two resonant frequencies plus beam theory can be used to deduce the modulus of the coating (see, for example, Kinbara *et al.* 1981). Secondly, the 'blister' or 'bulge' technique (see, for example, Yang *et al.* 1977; Bromley *et al.* 1983; Allen *et al.* 1987; Cardinale & Tustison 1990, 1991) in which a circular area of substrate is etched away and the area of coating (now only supported about its periphery) is pressurized; the modulus can be calculated from the film deflection. Thirdly, by indentation with a nano-indenter and analysis of the displacement records (for references, see §3*a*). Finally, by Brillouin scattering using similar techniques and analysis to that used by Grimsditch & Ramdas (1975) for single crystal diamonds.

The first two methods are the cheaper and most direct solutions and can obtain values to a few percent accuracy provided the experimenter is careful enough and the films are of greater thickness than, say, 10 μm on a millimetre thickness substrate. A nano-indenter is a relatively expensive piece of equipment and the interpretation of the data for moduli is more complex. The Brillouin technique is potentially the most accurate but needs sophisticated equipment and skilled interpretation.

The modulus as a function of temperature can be measured using the vibrating

PHILOSOPHICAL TRANSACTIONS OF THE ROYAL SOCIETY A MATHEMATICAL, PHYSICAL & ENGINEERING SCIENCES

Figure 2

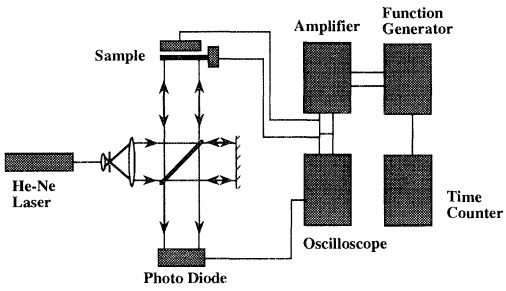

Figure 3

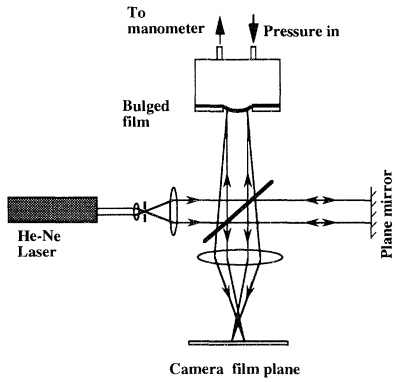

Figure 2. Schematic of the vibrating reed apparatus. At resonance the fringe visibility is lost and this is detected by the photodiode.

Figure 3. Schematic of the bulge test. Interference fringes allow the deflection of the membrane to be recorded.

need or 'blister' techniques provided a suitable furnace arrangement (with 'windows') is designed.

The vibrating reed apparatus used in our experiments is shown schematically in figure 2. The apparatus consists of two parts; vibration generation and frequency detection. The beams, of length 15–50 mm, width 3–5 mm are clamped to form part of a capacitor, with an aluminium reference electrode. A frequency function generator produces a variable frequency, sinusoidal voltage, which is amplified to a level required to cause the beam to vibrate. The vibrational frequency is detected using a Michelson's interferometer. A photodiode is placed behind a pin hole in the screen on to which the interference pattern falls. The pinhole is positioned at the edge of a bright fringe. At resonance, blurring out of the interference pattern occurs. This frequency is recorded and used to calculate the modulus of the beam.

In the case of very thin films, a composite beam is used. The modulus is calculated by first determining the resonant frequency of the substrate material (monolithic beam) and then repeating the experiment for the composite beam. It is from the shift in resonant frequency, that the Young's modulus of the film is calculated. In this way the modulus of deposited films as thin as a few tens of nanometers can be determined.

The Bulge test apparatus used in our experiments (figure 3) consists of a cylindrical chamber the front section of which has an opening of diameter greater than that of the membrane, through which the bulging of the film can be viewed. The sample is in the form of a 16 mm × 16 mm square of silicon coated with a hard thin film, with a circular membrane in the centre. A known pressure differential is applied across the membrane by means of a syringe. Pressures of up to 10^4 Pa (100 mbar) above atmosphere are produced within the chamber, which are measured using a manometer. A Michelson's interferometer is used to monitor the radius of curvature of the membrane. The central deflection of the membrane is found by counting the number of circular interference fringes formed as a function of pressure. Using this measurement, the radius of curvature of the membrane can be determined, from which the height of the bulge and hence the Young's modulus can be calculated. Because of diamonds extreme inertness to powerful etchants, an anisotropic etching

PHILOSOPHICAL TRANSACTIONS OF THE ROYAL SOCIETY A MATHEMATICAL, PHYSICAL & ENGINEERING SCIENCES

technique, involving concentrated etchants at room temperature was used. The etchant used was a 1:1 mixture of concentrated HF (40%) and HNO_3 (Cardinale & Tustison 1990, 1991). The etch time for each sample varied from 5–10 min depending on the thickness of the silicon substrate. The diameter of the membranes where circular to within approximately 0.06 of a mm for a 6–6.5 mm diameter membrane.

(*c*) *Thermal conductivity* (*diffusivity*)

The thermal 'mirage' technique used by Anthony *et al.* (1990) to measure the thermal conductivities of isotopically pure diamond have been applied to thin film conductivity measurements (Pryor *et al.* 1990). The technique essentially involves heating a surface volume with one laser pulse and then interrogating the heated gas layers above the surface with a second laser beam travelling parallel to the specimen surface. The published data shows an almost linear increase of diffusivity with decreasing graphite content. Ono *et al.* (1986) have shown that the thermal conductivity of diamond films decreases as the methane to hydrogen ratio increases with decreasing graphite.

(*d*) *Coefficient of expansion*

This can in theory be measured for unsupported films, but if they are very thin (a few to tens of micrometres) then buckling is a major problem. It appears to be better to observe the deflections of coated substrates (with the substrate relatively thin). A similar furnace set up can be used as for the modulus versus temperature measurements, with beam deflections giving expansion coefficients and beam vibration reasonances giving moduli.

(*e*) *Erosion properties*

Techniques are available at Cambridge for measuring the erosion resistance of materials to both solid particle and liquid drop impact. The solid particle impact apparatus uses gas flow to accelerate particles along a steel tube. The particles are fed into the flow from a reservoir using compressed air and the particle flux is controlled by means of a turntable in the reservoir. Impact velocities, which can be varied in the range up to *ca.* 300 m s^{-1}, are measured using a cross-correlation method to an accuracy of *ca.* 4%. Specimens can be mounted at any angle but normal incidence (i.e. 90°) was used in this work since this gives maximum erosion for 'brittle' materials. In the experiments on CVD films, the solid particles were sieved sand with dimensions of 300–600 μm and mean particle mass of 190 µg. The flux rate was 4.6 kg m^{-2} s^{-1} and impact velocities of 34 m s^{-1} and 59 m s^{-1} were chosen. Further details of the apparatus are given in Andrews *et al.* (1983) and Walley & Field (1987). Erosion data on bulk diamond and polycrystalline diamond composites (PDCs) are given in Hayward & Field (1990) and Feng & Field (1990).

Forward-facing aircraft components, particularly window materials, may suffer damage due to impact with rain drops. Materials coated with CVD diamond, or self-supporting CVD diamond layers themselves are currently under study as infrared transmitting windows.

Liquid impact studies have been in progress at Cambridge since the early work of Bowden & Brunton (1961) and Bowden & Field (1964). The key to understanding the pressure generated by liquid impact is the realization that there is always an initial regime where the contact edge velocity between liquid and target is higher than the shock wave velocities in the liquid and solid. This means that the liquid behind the

shock envelope behaves compressibly, giving pressures of order ρCV, where ρ is the liquid density, V the impact velocity and C the shock velocity in the liquid. It is only when the shock envelope overtakes the contact edge that release waves move into the liquid allowing incompressible flow and sideways jetting (Bowden & Field 1964; Lesser 1981; Lesser & Field 1983).

For the impact velocities likely to arise in most rain erosion situations, the ratio of compressible to incompressible pressures is very large (34 times at 100 m s^{-1}, 10 times at 500 m s^{-1}). In other words, it is the very early stages of liquid impact which are all important. Impacts by rain drops of a few 100 m s^{-1} produce pressures of gigapascal magnitude and submicrosecond duration followed by lateral outflow (jetting) at a few times the impact velocity. The fact that the early stage of liquid impact is all-important also allows drop impact to be simulated by firing liquid jets at stationary targets (a much simpler approach than projecting specimens at suspended drops), though it is essential to produce jets that are coherent and that have a smooth, slightly curved front profile. It is possible to calibrate jet impacts in terms of equivalent drop sizes which they reproduce (Field *et al.* 1979).

The rain erosion testing described in this paper has been performed with a multiple impact jet apparatus (MIJA). This produces a series of reproducible jets of chosen dimension and in the velocity range up to *ca.* 600 m s^{-1}. A computer-controlled specimen stage allows impacts to be coincident or in arrays or random patterns that are reproducible. The computer also records all relevant impact parameters including each impact velocity (Seward *et al.* 1990).

In *quantitative* studies of liquid impact it is important to be able to determine 'threshold velocities' for damage, i.e. the velocity at which a particular sized drop or jet causes strength loss in the target. With single impact testing, the threshold velocity can be determined by obtaining 'residual' strength curves, i.e measuring the specimen strength after impact, and recording the velocity at which strength loss takes place. This is much more accurate than recording the onset of visual damage (by eye or low power microscopy) since the defects controlling the strength may still be submicroscopic (see, for example, Field *et al.* 1979; van der Zwaag & Field 1983*b*). With MIJA , a different approach is used and the number of impacts to cause visible damage at a particular impact velocity is recorded (see later).

(*f*) *Frictional properties*

Friction measurements were made with an apparatus of the reciprocating type. A diamond stylus moves to and fro along a 1 mm track with a chosen load. Data are recorded at 10 μm separations, though the readings from the ends of the track where the stylus stops and reverses are not used. To avoid having to store too much data the computer is programmed to only record data when significant changes of friction coefficient occur. The programme allows the operator to abort or pause the experiment or to manually override the recorded algorithm and force the apparatus to take readings. For a full discussion, see Hayward & Field (1988).

4. Results

(*a*) *Hardness and modulus*

The Knoop hardness of natural diamond falls in the range 55–113 GPa depending on the crystal orientation and whether the diamond is type I or type II (see chapters by Brookes in Field 1979, 1992). The extreme hardness of diamond makes its

measurement difficult and skill is required if the indenter is not to be broken. The fact that CVD diamond can also damage indenters suggests that it can also be hard. A selection of our and other peoples data are given in table 1. Beetz *et al.* (1990) found that films deposited at lower methane concentration, 0.11 % CH_4 in H_2, had large crystallite sizes of 5–8 μm and an average hardness and modulus of 31 and 541 GPa respectively. A higher CH_4 concentration of 0.99 % in H_2 resulted in finer crystallites of *ca.* 0.5 μm and average hardness and modulus of 65 and 875 GPa respectively. According to Beetz *et al.* there is more Sp^3 bonding in the lower hardness film which is counter intuitive but changes in crystal size may be the dominant feature. (It is regretable that Beetz *et al.* compromize the value of their results by so many discrepancies between data in their figures and statements in the text.) Similar values of hardness and modulus were found for CVD films by Tsukamoto *et al.* (1987). Our own work and that of many authors have moduli values for CVD diamond in the range 700–900 GPa. Diamond-like carbon (DLC) films, as expected, tend to have lower hardness and modulus values (though note that a hardness of 20 GPa is still about three times that of tool steel!). The very high values (see table 1), close to the aggregate bulk value for diamond of 1041 GPa (Ruoff 1979) are surprising. In our experience, the bulge test can give high modulus values if the film has corrugations and this may be an important factor. The accuracy of the values obtained in the vibrating reed and bulge tests is not limited at present by the intrinsic accuracy of the tests (to a few percent), but by the imperfections of the films; non-uniformities in thickness, residual stresses, etc.

(*b*) *Erosion and strength*

(i) *Solid particle erosion*

The erosion resistances of bulk diamond and PCD composites are the highest yet recorded (Hayward & Field 1990; Feng & Field 1990; Vaughan & Ball 1991). With sand as the erodent, there is negligible erosion until velocities in excess of *ca.* 100 m s^{-1} and then the steady state erosion is at a rate of *ca.* 0.05 mg per kg of erodent. Bulk diamond first forms a network of cracks and material loss only starts when cracks intersect. Polycrystalline diamond composites erode primarily by loss of the binder metal (usually cobalt).

To date, four CVD films have been studied (Feng *et al.* 1992*a*); (*a*) polished film (with a surface roughness of 8 nm CLA and a film thickness of *ca.* 15 μm), deposited on a silicon nitride substrate by microwave plasma CVD; (*b*) unpolished film (with a surface roughness of 1 μm CLA and a film thickness of *ca.* 6 μm), deposited on silicon by hot filament CVD with (100) facets dominating; (*c*) unpolished film (the preparation method, surface roughness, thickness and substrate were the same as (*b*), but diamond grains with (111) facets dominating); and (*d*) unpolished free-standing film deposited by hot filament CVD with a grain size of 2–4 μm and a film thickness of 25 μm. Films (*a*), (*b*) and (*c*) were used in the solid impact experiments and film (*d*) for fractographic study following bending. Film (*a*) was also used in static indentation experiments to determine fracture strength and to make a comparison with results obtained from impact experiments. Detailed information about the preparations and characterizations of the CVD diamond films can be found in Srivinyonon *et al.* (1991) and Nishimura (1991).

In these erosion experiments impact velocity and exposure time were varied and the conditions for film cracking and delamination obtained. The first experiment was performed at an impact velocity of 59 m s^{-1}, with a flux rate of 4.6 kg m^{-2} s^{-1} and an

PHILOSOPHICAL TRANSACTIONS OF THE ROYAL SOCIETY A MATHEMATICAL, PHYSICAL & ENGINEERING SCIENCES

Table 1. *Thin film properties*

(HFA, hot filament assisted; MPA, microplasma assisted; P, plasma; DLC, diamond-like carbon; Si, silicon substrate.)

film type	hardness / GPa	modulus / GPa	measurement method	reference
MPACVD/Si		740 ± 20 (3.7 μm)	vibrating reed	this paper
(3–11 μm)		710 ± 20 (5.5 μm)		
MPACVD free standing				
(230–245 μm)		745 ± 10	vibrating reed	this paper
(150–180 μm)		780 ± 10		
MPACVD		680–790	vibrating membrane	Berry *et al.* (1990)
HFACVD/Si	31	540[a]	nano indentation	Beetz *et al.* (1990)
35 μm	65	875[b]		
MPACVD				
9.6 μm		864, 893[c]	bulge test	Cardinale & Tustison (1990, 1991)
16 μm		1054, 1095[c]		
DLC/Si	20–48	480–850	H = nano indentation for E = beam bending, with both end supported	Hoshino *et al.* (1989)
0.25–0.4 μm				
P CVD DLC/Si	63–67	810–820	H = nano indentation E = beam bending, with ends supported on fulcrums	Tsukamoto *et al.* (1987)
0.1–0.4 μm				

[a] Low % CH_4. [b] High % CH_4. [c] ν taken as 0.1 and 0.07 respectively.

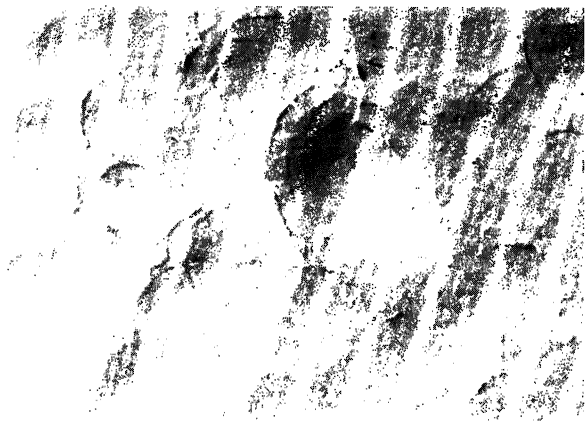

Figure 4. Optical micrographs of an eroded CVD diamond film at an impact velocity of 34 m s^{-1} for 10 s.

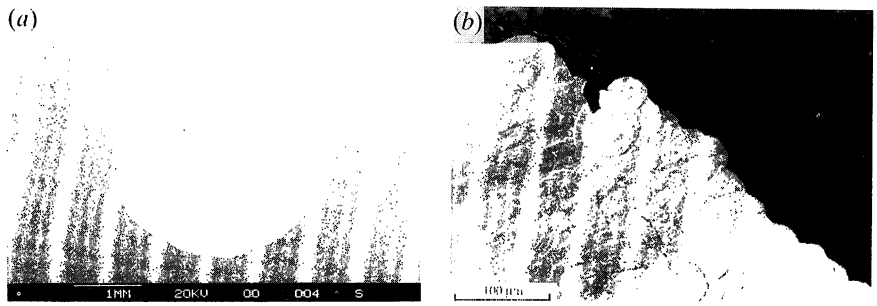

Figure 5. (*a*) Optical micrograph of an eroded CVD diamond film at an impact velocity of 59 m s^{-1} for 70 s. (*b*) SEM micrograph of an area near the broken edge.

exposure time of 10 s, and ring cracks were found on the surfaces after impact (see figure 4). The experiment was then carried out at a lower sand velocity, 34 m s^{-1}, with the same flux rate and for the same time of exposure, and again ring cracks were formed on the surfaces but with a lower crack density. There was no significant difference in the sizes of ring cracks observed at these two velocities. No diamond film removal occurred at this stage for either impact velocity. Experiments were then performed at an impact velocity of 59 m s^{-1} for an increased time of impact. It was found that film removal from the substrate started after an exposure time of *ca.* 70 s. Figure 5*a* shows an SEM micrograph of the area where the film was delaminated. Figure 5*b* is an optical micrograph from the edge of the impacted area and shows that the boundary is defined by the ring cracks. The film surface adjacent to a delaminated area can be used to study what happens just before film removal starts because of the lower impact flux in this area owing to the shadowing effect of the rubber mask. Examination by optical microscopy showed that the film surface became increasingly wavy compared with other areas. This is presumably due to partial debonding of the film from the substrate. The fractured edge tends to curve out of the substrate surface because of residual stresses in the film.

The damage process for a CVD diamond film by sand particle impact follows the sequence (i) formation of ring cracks, (ii) debonding and/or penetration of the film, and (iii) removal or delamination of the film from the substrate. The formation of

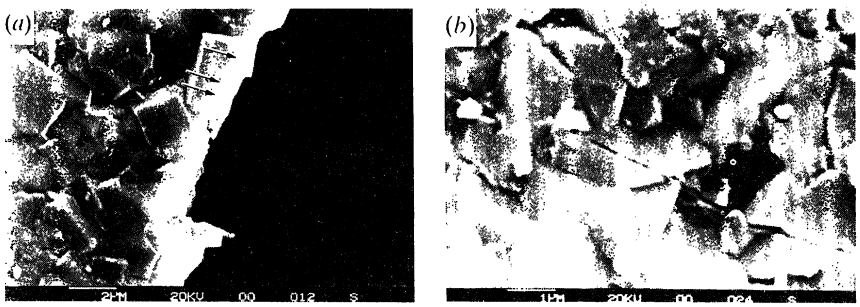

Figure 6. SEM micrographs of fractured surfaces produced by sand particle impact (*a*) on an unpolished (100) facet dominated film, (*b*) on an unpolished (111) facet dominated film. Both contain examples of transgranular fracture.

ring cracks at the initial stage is a typical fracture phenomenon for brittle materials. This was also observed in the impact of natural diamond by sand particles using the same apparatus (Feng & Field 1990). However, the material removal mechanisms are very different: in the case of CVD diamond, the premature removal of the film is caused by the delamination; while in the case of natural diamonds it occurs only when ring or cone cracks intersect to separate small volumes of diamond from the bulk.

(ii) *Fracture morphology and strength*

Scanning electron microscopy of the fracture surfaces of the eroded films and also CVD free-standing films showed many examples of transgranular fracture. Figure 6*a* shows a fractured edge on a (100) facet dominated film: the arrowed region clearly indicates transgranular fracture. Figure 6*b* shows a similar micrograph for a (111) facet dominated film. Transgranular fracture was also common when free-standing films were broken by bending.

The fracture strengths of the films were estimated (see Feng *et al.* (1992*a*) for full details) by measuring the ring crack diameters on the eroded specimens and assuming that they were formed by spherical sand particles of diameters in the range 300–600 μm. Additionally, ring cracks were formed by indenting with a 0.39 mm tungsten carbide sphere. In both cases, Hertz theory (elastic sphere indenting on elastic half-space) was used.

Both theory (El-Sherbiney & Halling 1976; van der Zwaag & Field 1982) and experiment show that for a hard coating with a Young's modulus about three times that of the substrate and a coating thickness of $d/a_0 \approx 0.5$ (where d is the coating thickness and a_0 the contact radius calculated by Hertz theory), the measured contact size on the coating is almost the same as that given by Hertz theory for a half-space of the coating material. The result of these measurements is that ring cracks form on CVD film at a critical contact pressure (load divided by crack area) of 3.2 GPa compared with a critical contact pressure of 10–13.5 GPa for natural diamond (data from Howes 1962). Assuming the ring crack propagates at 90° to the surface and that the Poisson ratio is 0.07 then Hertz theory predicts a tensile strength for CVD diamond of 1.4 GPa and 4–6 GPa for bulk natural diamonds. (Note Feng *et al.* (1992*a*) missed a factor 2 which gave their values twice as high as these.) Windischmann *et al.* (1991) recorded CVD strengths in the range 1–5 GPa using a bulge test.

PHILOSOPHICAL TRANSACTIONS OF THE ROYAL SOCIETY A MATHEMATICAL, PHYSICAL & ENGINEERING SCIENCES

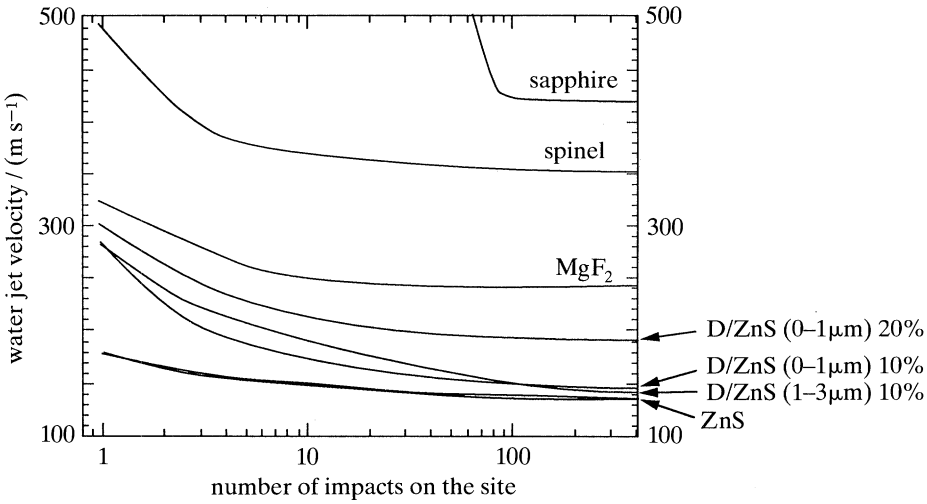

Figure 7. Liquid impact erosion data for a range of materials. A curve separates damaged and undamaged sites. The velocities after 400 impacts are taken as 'threshold' values. Data for a 0.8 mm nozzle.

Table 2. *Threshold data for liquid impact*
(MITV, multiple impact threshold velocity.)

material	MITV 0.8 mm jet/(m s^{-1})	MITV 2 mm drop/(m s^{-1})
zinc sulphide	130	190
magnesium fluoride	205	290
spinel	350	460
sapphire (25 mm disc)	420	*ca.* 535
natural diamond	*ca.* 530	*ca.* 600
amorphic diamond on ZnS (1 μm)	*ca.* 160	*ca.* 235
ZnS/D 20%, 0–1 μm	190	270
ZnS/D 10%, 1–3 μm	140	205
ZnS/D 10%, 0–1 μm	140	205
CVD diamond	< 200	< 285

(iii) *Liquid impact erosion*

Data on the liquid impact performance of a range of infrared transmitting materials are given in figure 7 and table 2. The MIJA was programmed to impact a succession of sites at different, pre-selected velocities (17 in the data illustrated in figure 7). The specimen, still on its computer-controlled stage was then moved for microscopic examination. The sites at which damage was visible were recorded. The procedure was then repeated for larger numbers of impacts with impacts on the original sites at the same pre-selected velocity. Microscopic examination was made regularly until undamaged sites had received 400 impacts. After this number of impacts it has been shown that sites where the 'threshold' velocity has been exceeded exhibit visual damage. Sites which do not show damage at this stage are below the critical threshold velocity.

Zinc sulphide, ZnS, is an important infrared window material in the 8–12 μm range but it is a relatively weak material with a low threshold for damage. It is interesting that ZnS strengthened by diamond particles has an improved erosion

PHILOSOPHICAL TRANSACTIONS OF THE ROYAL SOCIETY A MATHEMATICAL, PHYSICAL & ENGINEERING SCIENCES

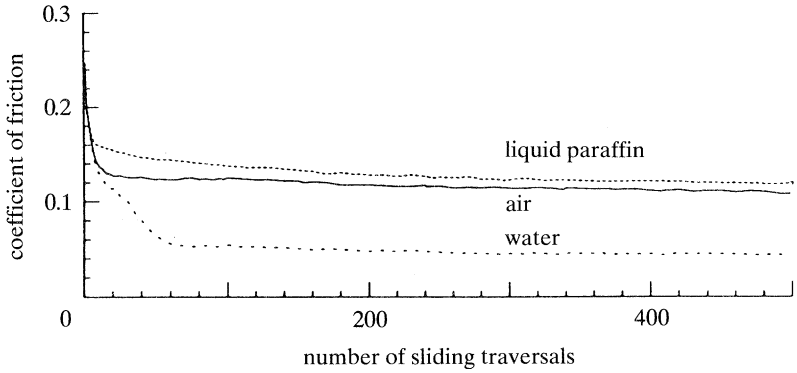

Figure 8. Frictional coefficient of diamond sliding on a CVD diamond coating against number of sliding traversals in air, liquid, paraffin and water.

response. (For details of how these composites are fabricated and their strength and optical properties see Xue *et al.* (1990) and Farquhar *et al.* (1990).)

Sapphire, germanium (Ge), magnesium fluoride and spinel have superior thresholds to ZnS but Ge has poor transmission above 370 K and the others are of prime interest in the 3–5 μm window range.

Rain erosion threshold velocity data on natural diamond are, not surprisingly, scarce. To date we have tested one natural diamond; a 6 mm diameter, 2 mm thick type IIa diamond. The threshold figure for impact by a 0.8 mm jet (equivalent to a 4 mm drop) was *ca.* 530 m s^{-1}. The equivalent 2 mm drop threshold, calculated by equations given in Hand *et al.* (1991), is *ca.* 600 m s^{-1}. This may be artificially low because of the small specimen size which would give sizeable reflected tensile pulses. In other experiments, amorphic diamond CVD coatings on ZnS detached at a velocity of *ca.* 160 m s^{-1} (2 mm drop equivalent of *ca.* 235 m s^{-1}). Experiments on a bulk CVD layer of 300 μm thickness had a threshold velocity of *ca.* 200 m s^{-1} (2 mm drop equivalent of *ca.* 285 m s^{-1}). However, it is likely that this specimen was considerably weakened by the presence of microcracks before testing, so this value is probably much lower than what could be achieved with a carefully selected specimen.

(iv) *Frictional properties*

The friction of natural diamond has been of considerable interest for many years due to its low value. The precise figure depends on the crystal force, the sliding direction, the material it slides against and the load. For diamond sliding on diamond, in air, values of 0.05 to 0.1 are common and in the presence of water can be even lower (for a recent review see Tabor & Field (1992)).

A potential advantage of CVD diamond is that the friction should be more isotropic with sliding direction. Research to date on CVD diamond has shown the following. (i) The friction coefficient is usually two or three times that of natural diamond for diamond sliding on diamond. Feng & Field (1992) have, for example, recorded values of *ca.* 0.25 for the friction coefficient of CVD diamond coated on silicon. This friction, for a small number of traversals, remained constant up to a load of 2N (contact pressure *ca.* 10 GPa) when coating delamination occurred. (ii) With large numbers of traversals, the coefficient of friction decreases (see figure 8). The higher initial value has been attributed to the greater surface roughness of the CVD diamond (Feng & Field 1991; Hayward *et al.* 1992). As the sliding progresses, the friction track

becomes smoother. (iii) The friction response to different oils (small effect) and to the pressure of water (large effect; see figure 8) is qualitatively the same as natural diamond (Feng & Field 1991). (iv) There is some evidence that at heavy loads the CVD layer is plastically deformed (Feng & Field 1991).

5. Discussion

The measurement of CVD diamond properties is at an early stage, but is essential if CVD coatings and self-supporting layers are to be optimized. Various techniques are available for modulus measurements, but as noted earlier, their value is limited less by the accuracy of the techniques than by problems with the films themselves. The measurements will become more meaningful as CVD layers become thicker, more uniform and less stressed.

We have recorded tensile strengths for CVD layers of *ca.* 1 GPa and this agrees with values by other workers. The value is less than for good quality diamond by a factor of 2–5 times. Field (1979) has estimated that sharp-ended microcracks of *ca.* 0.5 μm could explain the tensile strength of natural diamond. This would suggest flaws of *ca.* 2–10 μm in CVD diamond. The observation that *transgranular* fracture is common is encouraging since it suggests that the grain boundaries in CVD diamond can be strong.

The erosion and friction studies show that delamination can be a major problem. The potential of free-standing layers for infrared windows is exciting, since natural diamond has a very high erosion resistance against solid particles and a high threshold for damage for liquid drops. In the liquid impact test the threshold of natural diamond was probably artificially low because the small specimen size gives stress wave reinforcements from reflected waves. CVD layers would have similar thicknesses to natural diamond specimens and much greater lateral dimensions which would reduce this problem.

This work has been supported by grants from MOD Proc. Executive (now DRA) and De Beers Industrial Diamond Division. We thank De Beers, the Naval Research Laboratory, Washington, D.C., U.S.A., Professor Y. Tzeng, Auburn University, U.S.A. and Professor R. Raj, Cornell, U.S.A., for the provision of samples.

References

Allen, M. G., Mehregany, M., Howe, R. T. & Senturia, S. D. 1987 *Appl. Phys. Lett.* **51**, 241–243.

Andrews, D. R., Walley, S. M. & Field, J. E. 1983 In *Proc. 6th Int. Conf. on Erosion by liquid and solid impact* (ed. J. E. Field), paper 36. Cambridge: Cavendish Laboratory.

Anthony, T. R., Banholzer, W. F., Fleischer, J. F., Wei, L., Kuo, P. K., Thomas, R. L. & Pryor, R. W. 1990 *Phys. Rev.* B **42**, 1104–1111.

Beetz, C. P., Cooper, C. V., Perry, T. A. 1990 *J. Mater. Res.* **5**, 2555–2561.

Berry, B. S., Pritchet, W. C., Cuomo, J. J., Guarnieri, C. R. & Whitehair, S. J. 1990 *Appl. Phys. Lett.* **57**, 302–303.

Bowden, F. P. & Brunton, J. H. 1961 *Proc. R. Soc. Lond.* A **263**, 433–450.

Bowden, F. P. & Field, J. E. 1964 *Proc. R. Soc. Lond.* A **282**, 331–352.

Bromley, E. I., Randall, J. N., Flanders, D. C. & Mountain, R. W. 1983 *J. Vac. Sci. Technol.* B **1**, 1364–1366.

Brookes, C. A. 1979 In *The properties of diamond* (ed. J. E. Field), pp. 383–402. London: Academic Press.

Brookes, C. A. 1992 In *The properties of natural and synthetic diamond* (ed. J. E. Field), pp. 515–546. London: Academic Press.

PHILOSOPHICAL TRANSACTIONS OF THE ROYAL SOCIETY A MATHEMATICAL, PHYSICAL & ENGINEERING SCIENCES

Cardinale, G. F. & Tustison, R. W. 1990 *SPIE*, 1325, Diamond Optics III, 90–98.
Cardinale, G. F. & Tustison, R. W. 1991 *J. Vac. Sci. Technol.* A **9**, 2204–2208.
Davidson, J. L., Ramesham, R. & Ellis, C. 1990 *J. electrochem. Soc.* **137**, 3203–3205.
El-Sherbiney, M. G. D. & Halling, J. 1976 *Wear* **40**, 325–337.
Farquhar, D. S., Raj, R., Phoenix, S. L. 1990 *J. Am. Ceram. Soc.* **73**, 3074–3080.
Feng, Z. & Field, J. E. 1990 *J. Hard. Mater.* **1**, 273–287.
Feng, Z. & Field, J. E. 1991 *Surf. Coatings Technol.* **47**, 631–645.
Feng, Z. & Field, J. E. 1992 *J. Phys.* D **25**, A33–A37.
Feng, Z., Tzeng, Y. & Field, J. E. 1992*a* *Thin Solid Films* **212**, 35–42.
Feng, Z., Tzeng, Y. & Field, J. E. 1992*b* *J. Phys.* D **25**, 1418–1424.
Field, J. E. 1979 *The properties of diamond* (ed. J. E. Field). London: Academic Press.
Field, J. E. 1992 *The properties of natural and synthetic diamond* (ed. J. E. Field). London: Academic Press.
Field, J. E., Gorham, D. A., Hagan, J. T., Matthewson, M. J., Swain, M. V. & van der Zwaag, S. 1979 In *Proc. 5th Int. Conf. on Erosion by Liquid and Solid Impact* (ed. J. E. Field), paper 13. Cambridge: Cavendish Laboratory.
Grimsditch, M. H. & Ramdas, A. K. 1975 *Phys. Rev.* B **11**, 3139–3148.
Hand, R. J., Field, J. E. & Townsend, D. 1991 *J. appl. Phys.* **70**, 7111–7118.
Hayward, I. P. & Field, J. E. 1988 *J. Phys.* E **21**, 753–756.
Hayward, I. P. & Field, J. E. 1990 *J. Hard. Mater.* **1**, 53–64.
Hayward, I. P., Singer, I. L. & Seitzmann, L. E. 1992 *Wear* **157**, 215–228.
Hoshino, S., Fujini, K., Shohata, N., Yamaguchi, H., Tsukamoto, Y. & Yanagisawa, M. 1989 *J. appl. Phys.* **65**, 1918–1922.
Howes, V. R. 1962 *Proc. Phys. Soc.* **80**, 78–80.
Isukamoto, Y., Yamaguchi, H. & Yanagisawa, M. 1987 *Thin Solid Films* **154**, 171–181.
Kinbara, A., Baba, S., Matuda, N. & Takamisawa, K. 1981 *Thin Solid Films* **84**, 205–212.
Lesser, M. B. 1981 *Proc. R. Soc. Lond.* A **377**, 289–308.
Lesser, M. B. & Field, J. E. 1983 *A. Rev. Fluid. Mech.* **15**, 97–122.
McHargue, C. J. 1990 *Proc. NATO Adv. Study. Inst.* Italy, Plenum Press.
Nishimura, K. 1991 *Diamond Optics IV SPIE* **1534**, 199–205.
Oliver, W. C. & McHargue, C. J. 1988 *Thin Solid Films* **161**, 117–122.
Ono, A., Baba, T., Funamoto, H. & Nishihawa, A. 1986 *Jap. J. appl. Phys.* **25**, L808–810.
Pethica, J. B., Hutchings, R. & Oliver, W. C. 1983 *Phil. Mag.* A **48**, 593–606.
Pryor, R. W., Kuo, P. K., Wei, L. & Thomas, R. L. 1990 *Rev. Prog. Quant. NDE* **9**, 1123–1128.
Ruoff, A. L. 1979 In *High pressure science and technology* (ed. K. D. Timmerhaus & M. S. Barker), vol. 2, pp. 525–548. Plenum.
Seward, C. R., Pickles, C. S. J. & Field, J. E. 1990 In *Proc. SPIE Conf.* on *Window and Dome Technologies and Materials*, vol. 1326, pp. 280–290.
Smith, J., Holiday, P., Dehbi-Alaoui, A. & Mathews, A. 1992 *Diamond Related Mater.* **1**, 355–359.
Srivinyonon, T., Philips, R., Cutshaw, C., Joseph, A. J. & Tzeng, Y. 1991 In *Proc. 2nd Int. Conf. on New Diamond Science and Technology*, pp. 581–586. Pittsburgh: Materials Research Society. PA.
Tabor, D. & Field, J. E. 1992 In *The properties of natural and synthetic diamond* (ed. J. E. Field), pp. 547–571. London: Academic Press.
Tsukamoto, Y., Yamaguchi, H. & Yanagisawa, M. 1987 *Thin Solid Films* **154**, 171–181.
van der Zwaag, S. & Field, J. E. 1982 *Phil. Mag.* A **46**, 133–150.
van der Zwaag, S. & Field, J. E. 1983*a* *Phil. Mag.* A **48**, 767–777.
van der Zwaag, S. & Field, J. E. 1983*b* *Engng Frac. Mech.* **17**, 367–379.
van der Zwaag, S., Dear, J. P. & Field, J. E. 1986 *Phil. Mag.* A **53**, 101–111.
Vaughan, R. A. & Ball, A. 1991 *J. Hard. Mater.* **2**, 257–269.

PHILOSOPHICAL TRANSACTIONS OF THE ROYAL SOCIETY A MATHEMATICAL, PHYSICAL & ENGINEERING SCIENCES

Walley, S. M. & Field, J. E. 1987 *Phil. Trans. R. Soc. Lond.* A **321**, 277–303.

Windischmann, H., Epps, G. F. & Ceasar, G. P. 1991 In *Proc. 2nd Int Conf. on New Diamond Science and Technology*, pp. 762–772. Pittsburgh: Materials Research Society.

Xue, L. A., Farquhar, D. S., Noh, T. W., Sievers, A. J. & Raj, R. 1990 *Acta metall. Mater.* **38**, 1743–1752.

Yang, W. M. C., Tsakalakos, T. & Hilliard, J. E. 1977 *J. appl. Phys.* **48**, 876–879.

Discussion

L. M. Brown (*Cavendish Laboratory, Cambridge, U.K.*): It is an interesting observation that polycrystalline diamond films show largely transgranular fracture. Two influences may be at work here. First, if there is an intergranular layer of amorphous carbon it may provide some local plasticity and therefore a higher work of fracture for intergranular cracks than for transgranular ones, which will experience little or no plastic blunting. Secondly, I have the impression that in many films the diamond grains experience large internal stresses. Certainly, the multiply-twinned grains will have a strong circumferential tension at the external surfaces, unless plastic relief of stresses has occurred. The grains should be individually very fragile. Perhaps these two factors operate to explain the observed mode of fracture.

J. E. Field. Certainly it is encouraging that the grain boundaries are not major sources of weakness.

J. E. Butler (*Naval Research Laboratory, Washington, D.C., U.S.A.*): (*a*) Has the coefficient of friction been measured using other oxygen containing lubricants, e.g. alcohols, ketones, etc.? (*b*) Please comment on the role of tribochemical polishing of rough surface asperities by oxygen species on the lowering of the fraction coefficient? (*c*) Please comment on the degree to which the bulk mechanical properties of polycrystalline CVD diamond is controlled by the nature of the grain boundaries versus the defects in the individual grains?

J. E. Field. To date we have studied conventional lubricants and water, which, as shown in the paper, has a dramatic effect in reducing friction. At present, we are doing experiments with water at different pH values. I agree it would be useful to study oxygen-containing lubricants. It is difficult to comment briefly on the effect of surface roughness on diamond friction since there is still controversy about the mechanisms which operate in diamond friction (see Tabor & Field 1992). However, research at Cambridge and also at your laboratory has shown clearly that the coefficient of friction reduces as the diamond surface becomes smooth. My answer to Professor Brown gives our current thinking on question (*c*).

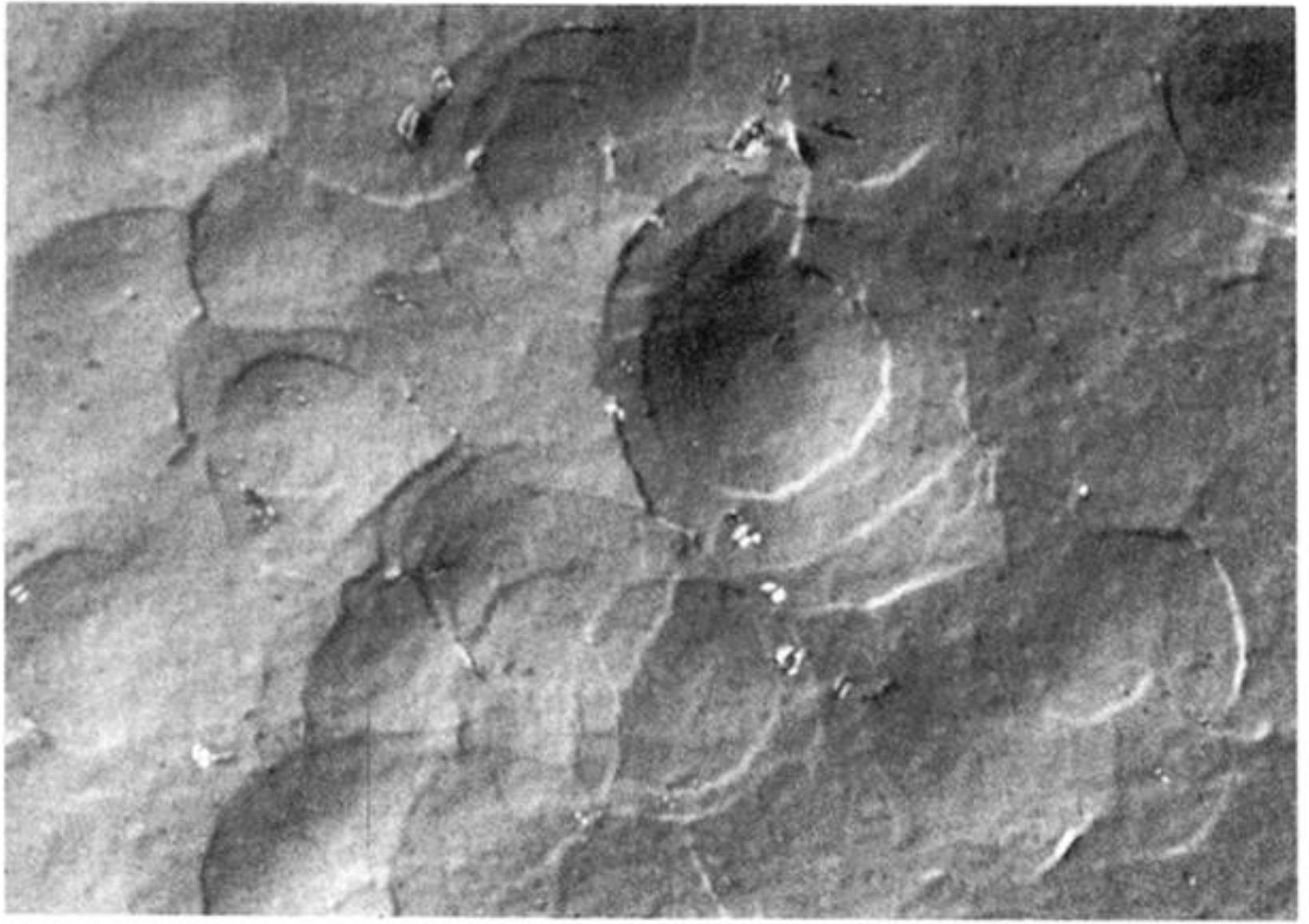

gure 4. Optical micrographs of an eroded CVD diamond film at an impact velocity of 34 m s^{-1} for 10 s.

PHILOSOPHICAL TRANSACTIONS OF THE ROYAL SOCIETY

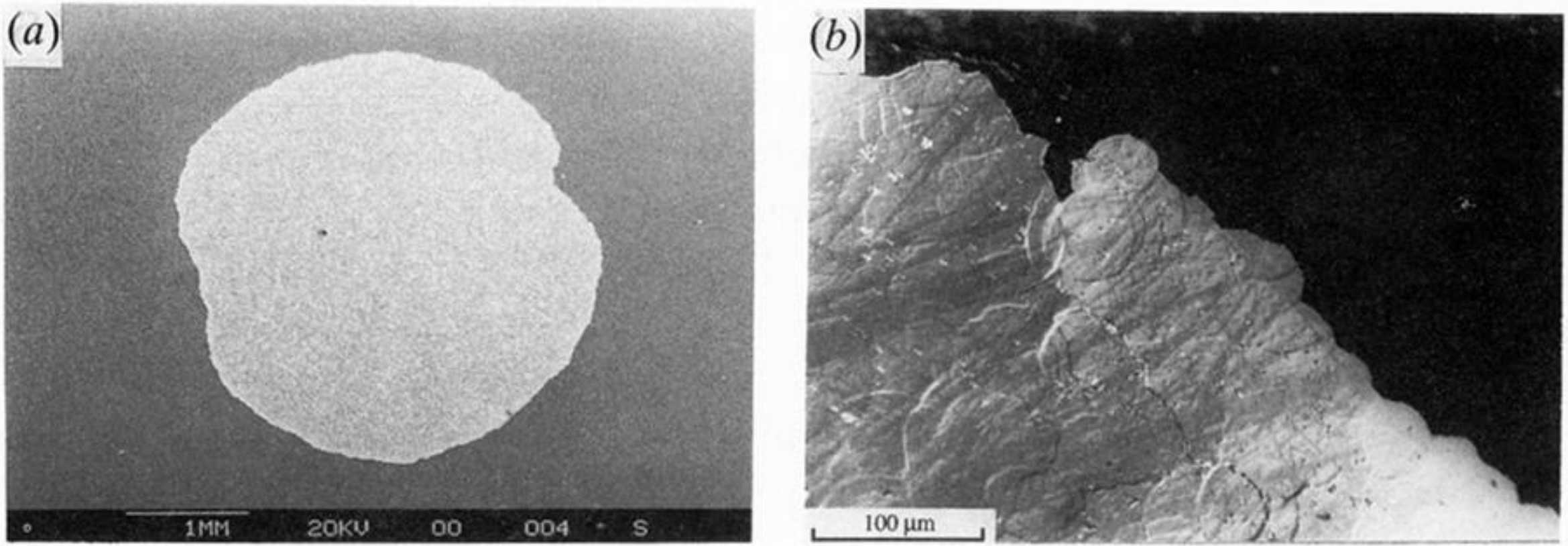

gure 5. (*a*) Optical micrograph of an eroded CVD diamond film at an impact velocity of 59 m s^{-1} for 70 s. (*b*) SEM micrograph of an area near the broken edge.

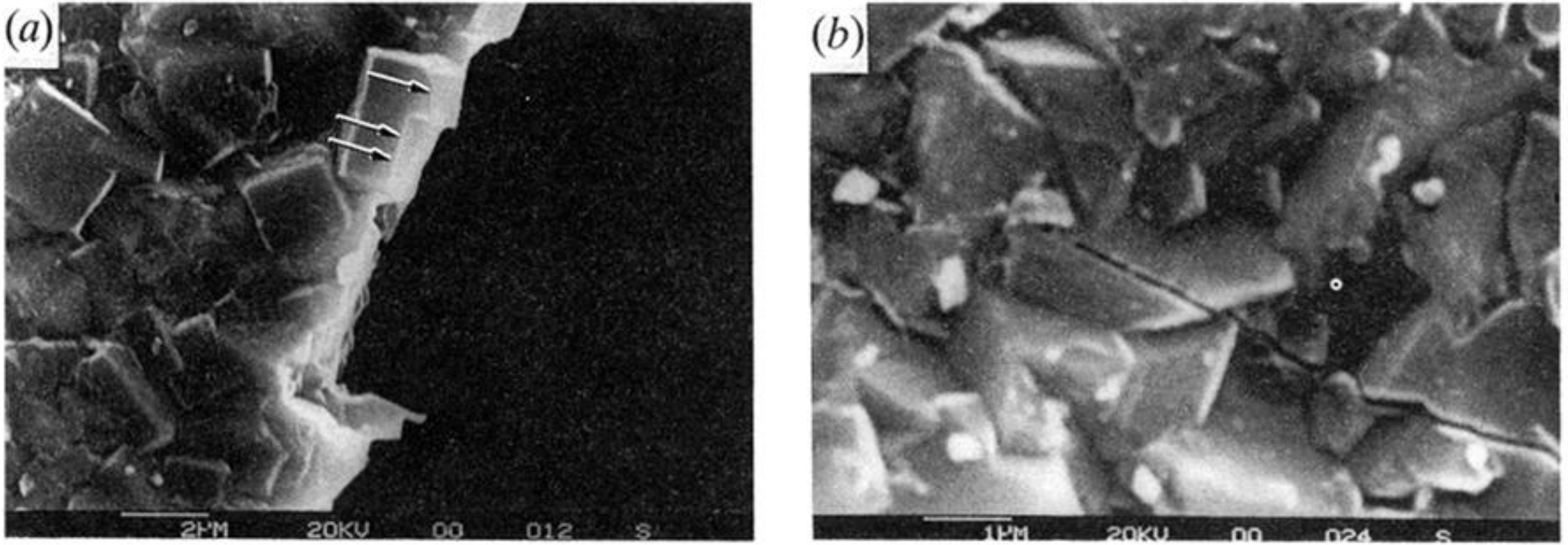

gure 6. SEM micrographs of fractured surfaces produced by sand particle impact (*a*) on an npolished (100) facet dominated film, (*b*) on an unpolished (111) facet dominated film. Both ntain examples of transgranular fracture.